

# Minima Timing of Eclipsing Binaries

Luboš Brát<sup>1</sup>, Zdeněk Mikulášek<sup>2,3</sup> and Ondřej Pejcha<sup>4</sup>

<sup>1</sup> Variable Star and Exoplanet Section of the Czech Astronomical Society; brat@pod.snezkou.cz

<sup>2</sup> Department of Theoretical Physics and Astrophysics, Masaryk University, Kotlářská 2, 611 37 Brno, Czech Republic; mikulas@physics.muni.cz

<sup>3</sup> Observatory and Planetarium of J. Palisa, VŠB-Technical University, Ostrava, Czech Republic

<sup>4</sup> Department of Astronomy, The Ohio State University, 140 West 18th Avenue, Columbus, OH 43210, USA; pejcha@astronomy.ohio-state.edu

## 1 Introduction

The minima timing of eclipsing binaries have long been used to learn about the dynamics of multiple stellar systems. Although the interest in this field continues, the methodology of obtaining accurate minima timings and their uncertainties is rooted long in the past. Specifically, the method of Kwee & van Woerden (1956) has enjoyed widespread use but is based on methods that are still several decades older. Conversely, the interest in transiting exoplanets in the last few years has produced more understanding of the data and more sophisticated methods of data analysis than what has been achieved in the field of eclipsing binaries in the past decades. The field of eclipsing binaries can benefit from the progress in the studies of transiting exoplanets.

In this paper, we describe our solution to the problem of minima timing of eclipsing binaries that is implemented on the website of the Variable Star and Exoplanet Section of the Czech Astronomical Society<sup>1</sup>. In Section 2, we describe the ideal solution to this problem, which we simplify in Section 3. In Section 4, we describe the calculation of uncertainties. In Section 5, we offer several recommendations for the usage of the on-line fitting tool.

## 2 Ideal situation

In the best possible case, we have enough data to completely cover all phases of the light curve. This makes it possible to construct a model of the eclipsing binary light curve. This is often done by minimizing the sum of square differences  $\chi^2$  between the magnitudes  $m_i$  with uncertainties  $\sigma_i$  at times  $t_i$  and the model  $f$ :

$$\chi^2 = \sum_{i=1}^{N_{\text{data}}} \left( \frac{m_i - f(t_i, \boldsymbol{\theta})}{\sigma_i} \right)^2. \quad (1)$$

Here,  $N_{\text{data}}$  is the total number of data points and  $\boldsymbol{\theta}$  is the set of model parameters. This includes not only the physical parameters of the binary and its orbit but also any incidental parameters of the data that describe systematic offsets and trends. If we desire to obtain minima timings from any future dataset, we can use the physical parameters of the binary to construct a template light curve and shift this light curve in time (and potentially also in magnitude to correct for systematic offsets) to derive the minimum timing. In other words, keeping physical parameters fixed and varying only the zero-point in time and data-specific parameters. In this way, a “minimum time” can be derived even from a dataset that does not cover the moment of conjunction – all data points with non-zero time derivative contribute to the “minimum time” determination.

However, there is a number of difficulties in implementing this ideal approach to real data that were obtained solely for the purpose of minima timings by amateur astronomers. Specifically, a single star is observed by the same observer only sporadically and observations are obtained only in the vicinity of one of the conjunctions. The parts of the light curve with nearly constant brightness are skipped. This poses great challenges for obtaining the model of the binary, especially when each of the little pieces has potentially different systematic trends and spectral response of the observation equipment. This would be exaggerated by combining data from different observers. While developing such a global model is conceivable, the amount of necessary effort and time far exceeds what is available to the authors<sup>2</sup>.

## 3 Our approach

Instead of the full model described in Section 2, we decided to take a more modest route. We abandon the goal of piecing all data together through a realistic model and fit each dataset separately. The improvement over the Kwee & van Woerden (1956) method lies in more thorough application of statistical techniques and more sophisticated estimation of parameter uncertainties.

---

<sup>1</sup><http://var.astro.cz>

<sup>2</sup>Any contribution toward this goal is warmly welcome and if you want to help, please contact us.

In our approach, the segment of the light curve around the minimum is modeled by function

$$f(t_i, \boldsymbol{\theta}) = c_0 + c_1 \psi(t_i, t_0, d, \Gamma), \quad (2)$$

where  $c_0$  is the magnitude zero-point shift and  $c_1$  is a constant that multiplies the profile of the eclipse

$$\psi(t_i, t_0, d, \Gamma) = 1 - \left\{ 1 - \exp \left[ 1 - \cosh \left( \frac{t_i - t_0}{d} \right) \right] \right\}^\Gamma. \quad (3)$$

Here,  $t_0$  is the time of minimum we seek,  $d > 0$  is the minimum width and  $\Gamma > 0$  specifies the pointedness of the minimum:  $\Gamma > 1$  corresponds to flat minima (total eclipses). The parameters minimized in the fit are  $\{c_0, c_1, t_0, d, \Gamma\} \in \boldsymbol{\theta}$ .

Equation (3) is a phenomenological description of the eclipse shape from Mikulášek (xxxx) and does not include any description of the light curve outside eclipse<sup>3</sup>. The parameters  $\boldsymbol{\theta}$  are different for each minimum even for the same star. This has two immediate consequences of great importance for the practical usage of the final tool:

- 
- **For minimum determination, always select interval that does not include any part of the light curve outside of the eclipse.** Obviously this means that constant parts of the light curve should not be included. These do not carry any weight for minimum determination anyway. Also, **avoid parts of the light curve dominated by proximity effects** caused by non-spherical shape of the stars, spots etc. You can often recognize these parts by a break in otherwise smooth ascending or descending branch.
  - **Select the fitting interval to be symmetric around the expected time of minimum.** If the observed ascending and descending branches do not have the same length, there might be a temptation to improve the fit by fully including the longer branch. The fit might be good and the minimum timing uncertainty might often decrease. However, the eclipse profile assumed in Equation (3) is not completely versatile and by using it to fit data that do not have a symmetric counterpart on the other branch you make an assumption that it is correct. We found that **using the fitting for asymmetric intervals can produce artificial offsets of more than 0.001 days** even when the uncertainty is formally smaller than that.
- 

We fit the data to Equation (2) by minimizing the  $\chi^2$  using the publicly-available nonlinear least squares routine `cmpfit`<sup>4</sup> (Moré 1978; Markwardt 2009). We calculate numerically the derivatives with respect to  $t_0$ ,  $d$  and  $\Gamma$ , while derivatives with respect to  $c_0$  and  $c_1$  are calculated analytically. The fitting routine is implemented in C and is multi-threaded using `OpenMP`.

## 4 Uncertainty estimation

Crucial part of any measurement is the estimate of the measurement uncertainty. This is especially important for minima time determination because the period analysis relies on understanding a diverse dataset obtained with different techniques and observers over decades. Reliable uncertainties are crucial in judging the credibility of the claimed effects such as apsidal motion, light-travel time and others.

Traditionally, the parameter uncertainties in least squares fitting are obtained from the diagonal elements of the covariance matrix. Such uncertainties, however, rely on the fact that measurement uncertainties  $\sigma_i$  in Equation (1) correctly describe the data. Photometric measurement uncertainties are often calculated as a combination of Poisson statistical error and known noise associated with the readout of the detector. However, additional sources of error might be present or the photometric error is calculated incorrectly (for example because incorrect detector parameters were entered in the reduction software). Sometimes, the observers report photometric series without any error bars.

In our approach, we still provide the uncertainties obtained from the least-squares fitting. Additionally, we provide uncertainty estimates obtained with more robust methods: bootstrapping and “prayer bead”, which are sometimes used in the exoplanet transit community. The more sophisticated techniques allow us to report not only the usual  $1\sigma$  uncertainties but generally asymmetric confidence intervals by analyzing the probability distributions of the parameters.

### 4.1 Bootstrapping

In ideal case, we would determine the uncertainties by analyzing many different sets of the data that were obtained simultaneously with the same equipment. In other words, by analyzing more samples from the same probability distribution. However, the properties of this distribution are unknown. Bootstrapping attempts to solve this problem by sampling the distribution using the original data: data points are randomly drawn from the original dataset, allowing for repeats. At each dataset, best fit model is calculated, best-fit parameters recorded and the whole process is repeated many times. The final parameter uncertainties are obtained from the cumulative distribution of individual parameters. To summarize, the algorithm can be represented as

---

<sup>3</sup>We tried to implement a more physical model based on a disk transiting a limb-darkened disk, where the functional form is also analytic through elliptic integrals. This problem was solved by Mandel & Agol (2002), while Pál (2008) later provided generalization to arbitrary disk sizes and analytic partial derivatives with respect to all parameters. In this model the parameters are  $t_0$ ,  $d$ , impact parameter, relative radii, and the relative flux ratio of the disks. Limb darkening coefficients are fixed. Unfortunately, even with analytic derivatives this model is about ten times slower than Equation (3) and is prone to severe degeneracies and does not converge well when only a part of the minimum is observed. We therefore choose to use Equation (3).

<sup>4</sup><http://cow.physics.wisc.edu/~craigm/idl/cmpfit.html>

```

for j=1 to j=N_bootstrap begin
  for i=1 to i=N_data begin
    k = random integer between 1 and N_data
    t_new[i] = t_original[k]
    m_new[i] = m_original[k]
    sigma_new[i] = sigma_original[k]
  end for
  new_theta[j] = best-fit parameter vector using t_new, m_new and sigma_new
end for
uncertainty = analysis of vectors new_theta

```

This algorithm does not make any use of the least-squares uncertainties and only uses the ratio of photometric measurement uncertainties, if available. Usually, the photometric uncertainties are underestimated so bootstrapping yields larger uncertainties than those from the least squares.

## 4.2 Prayer bead

In ideal case, the measurements are distributed randomly around the expect value and subsequent measurements are not correlated. Alternatively, this property can be expressed in terms of the Fourier transform of the residuals, which should have same power in all frequencies, “white noise”. However, real measurements often suffer from “red noise”, which has higher power in longer frequencies of the residuals. This usually manifests by having several consecutive measurements above or below the expected value. Red noise can potentially affect the determination of the minimum time and other parameters.

In order to estimate the influence of red noise, we employ the method of “prayer beads” that is sometimes used in the research of exoplanet transits (e.g. Pont et al. 2006; Gillon et al. 2007; Southworth 2008; Désert et al. 2011). In this method, the residuals are repeatedly shifted and applied to the original data while keeping track of the fitted parameters at each step. The algorithm can be written as

```

for i=1 to i=N_data begin
  residuals[i] = m[i] - best_fit_model[i]
end for

for j=1 to j=N_data begin
  for i=1 to i=N_data begin
    t_new[i] = t_original[i];
    sigma_new[i] = sigma_original[i];
    if (i < (N_data-j)) begin
      m_new[i] = m_original[i]+residuals[i+j];;
    end else begin
      m_new[i] = m_original[i]+residuals[i-N_data+j];
    end else
  end for
  new_theta[j] = best-fit parameter vector using t_new, m_new and sigma_new
end for
uncertainty = analysis of vectors new_theta

```

Clearly, the precision of the confidence intervals will be limited for small  $N_{\text{data}}$ . As a result, the prayer bead method should serve only as a check of the presence of the red noise.

## 5 Interpretation of the results

In this Section, we discuss some practical aspects of the fitting tool. Two recommendations were already given in Section 3.

- 
- **Always upload data with photometric uncertainties** because only then will have  $\chi^2$  any meaning. The expected value of  $\chi^2$  is equal to the number of degrees of freedom (DOF, the total number of datapoints minus the number of fitted parameters). Usually, the number of observations is much higher than of the fitted parameters. The expected standard deviation around the mean value is  $\sqrt{2\text{DOF}}$ , it is expected that  $\chi^2 \approx \text{DOF} \pm \sqrt{2\text{DOF}}$ . If  $\chi^2 \gg \text{DOF}$  then the photometric errors are underestimated or there is significant red noise or the model does not adequately fit the data. Conversely, if  $\chi^2 \ll \text{DOF}$ , then the photometric errors are likely overestimated.
  - The important consequence of the properties of  $\chi^2$  distribution is that the fitted **least-square parameter uncertainties are appropriate only if  $\chi^2 \approx \text{DOF}$** .
  - As a consequence, the **primary uncertainties of the parameters should be those from the bootstrap analysis**. Bootstrapping has its short-comings as well in the sense that it is also optimistic in the reported uncertainties. However, we find that for most datasets the bootstrapped uncertainties are larger than those from least-squares.

- We find that the prayer bead method is useful only as an indicator of the presence of the red noise and not as means to obtain parameter uncertainties. Because the number of resamplings is always equal to  $N_{\text{data}}$ , which can be quite small, the precision of the results is lower. The statistical properties of the prayer bead are also not fully understood. Therefore, **red noise likely affects the results if prayer bead uncertainties are greater than bootstrapped uncertainties**. Conversely, if the prayer bead uncertainties are smaller than bootstrapped uncertainties, no firm conclusion can be drawn. Fake red noise can be present if the model is inadequate for the data.
  - Bootstrapping (and to some extent also prayer bead) provides the full probability distribution of the fitted parameters. This allows us to calculate arbitrary confidence intervals on the parameters. The least squares method makes an implicit assumption that the distribution is Gaussian and characterized by the width  $\sigma$ . This means that in  $\sim 68.3\%$  of the cases the parameter falls within  $(\mu - \sigma, \mu + \sigma)$  confidence interval around the mean value  $\mu$ . To better characterize the asymmetry of the distribution we also calculate the 95% confidence interval, which approximately corresponds to  $\pm 2\sigma$  in case of a Gaussian distribution. **We report the result in the form  $\mu_{-b}^{+a}$ , which means that 95% of the results fall in the interval  $(\mu - b, \mu + a)$ , where  $\mu$  is the best-fit parameter value of the original dataset. If  $a$  is very different from  $b$ , the distribution is asymmetric.** One of the possible reasons is that the time of minimum determination depends heavily on a small number of datapoints. If these datapoints are removed, the result can be vastly different and the distribution becomes asymmetric. **This happens especially if there is only a handful of measurements on either the ascending or the descending branch.** The interpretation is that the minimum could have occurred much earlier (if  $a \ll b$ ) or later ( $a \gg b$ ).
- 

## 6 Credit

If you find our on-line fitting tool useful please cite

- **this paper**  
for the general description and web interface
- **Mikulášek (xxxx)**  
for the fitting function
- **Cagaš & Pejcha (2012)**  
for the fitting code and implementation of bootstrap analysis
- **Southworth (2008), Gillon et al. (2007) or other references mentioned in Section 4.2**  
for the prayer bead method

## References

- Cagaš, P., & Pejcha, O. 2012, A&A, 544, L3  
 Désert, J.-M., Sing, D., Vidal-Madjar, A., et al. 2011, A&A, 526, A12  
 Kwee, K. K., & van Woerden, H. 1956, Bull. Astron. Inst. Netherlands, 12, 327  
 Gillon, M., Demory, B.-O., Barman, T., et al. 2007, A&A, 471, L51  
 Mandel, K., & Agol, E. 2002, ApJ, 580, L171  
 Markwardt, C. B. 2009, Astronomical Data Analysis Software and Systems XVIII, 411, 251  
 Mikulášek, Z., some journal  
 Moré, J. 1978, in Numerical Analysis, vol. 630, ed. G. A. Watson (Springer-Verlag: Berlin), p. 105  
 Pál, A. 2008, MNRAS, 390, 281  
 Pont, F., Zucker, S., & Queloz, D. 2006, MNRAS, 373, 231  
 Southworth, J. 2008, MNRAS, 386, 1644

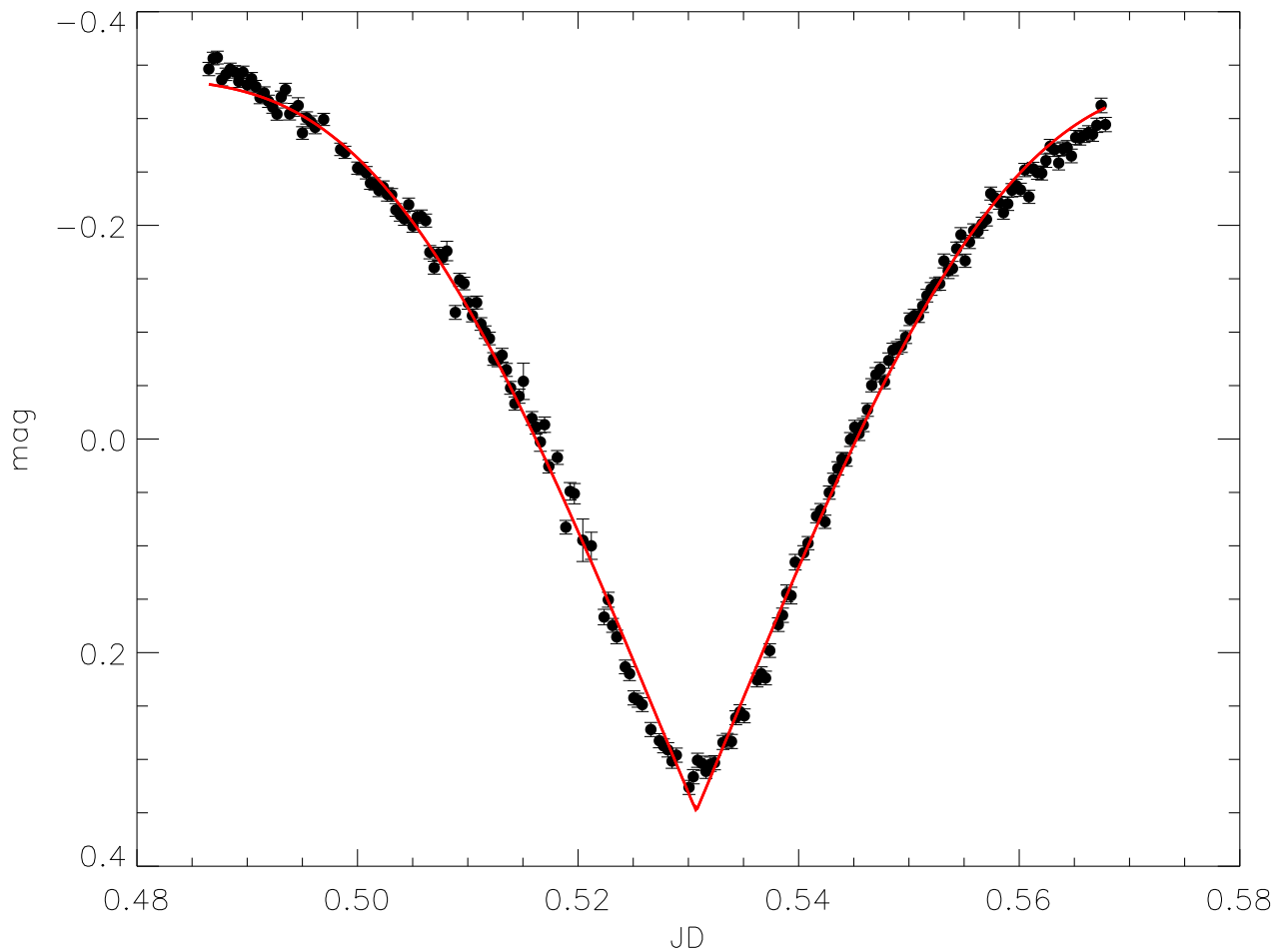


Figure 1: An example of a fitted light curve of V523 Cas from 9.7.2012 by K. Hoňková and J. Juryšek. The parameters of the fit are  $\chi^2 = 847$  for 182 DOF. The bootstrapped uncertainties are higher by about a factor of 2.5 than uncertainties from least squares. Note that the fit at minimum is not very good, but these measurements do not contribute much to the minimum determination anyway.

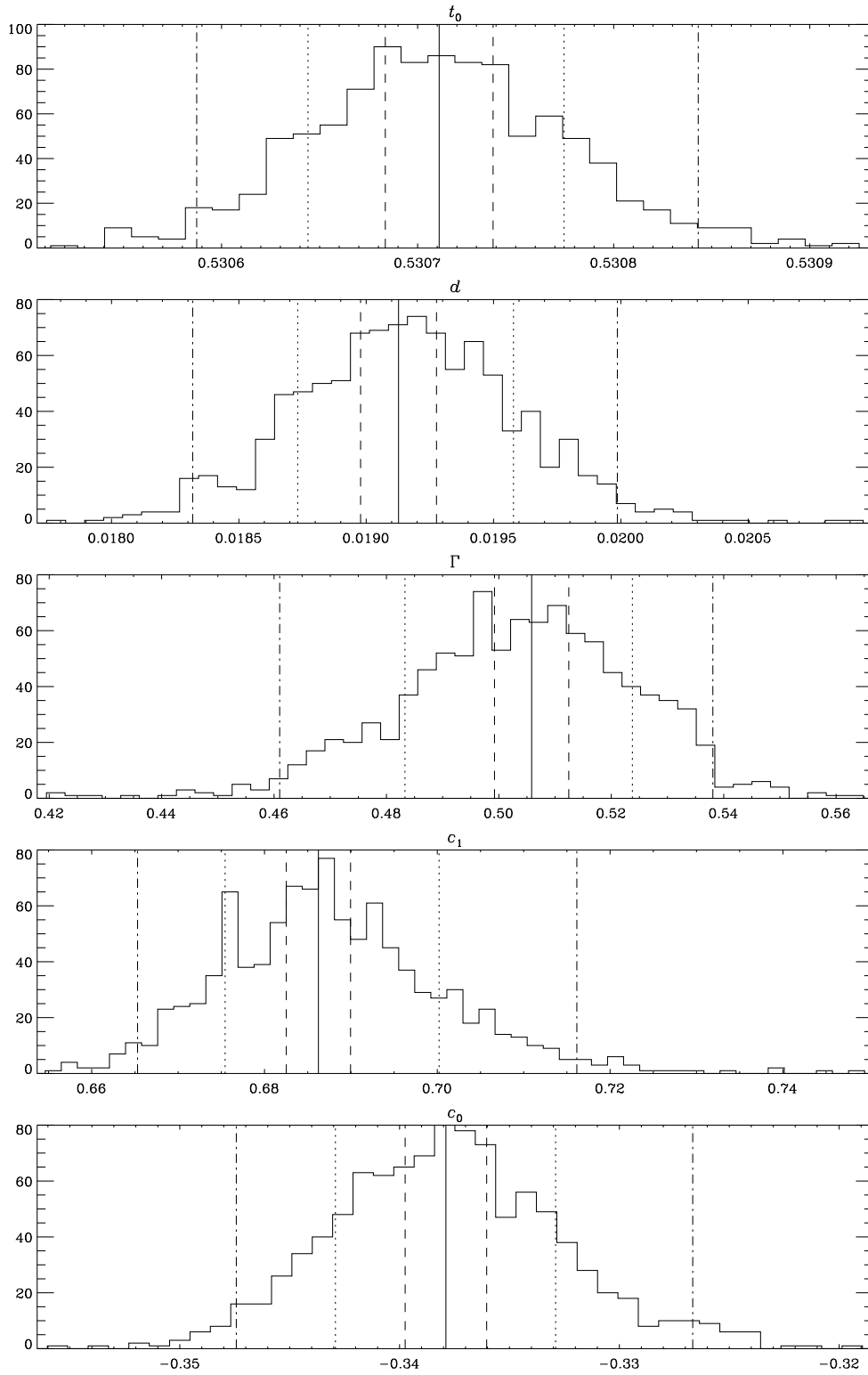


Figure 2: The probability distributions of the fitted parameters (solid histograms) from Figure 1. Vertical lines show the best-fit values from the original dataset (solid), least-squares  $1\sigma$  uncertainties (dashed), bootstrapped  $1\sigma$  uncertainties (dotted), and bootstrapped 95% confidence interval (dash-dotted).

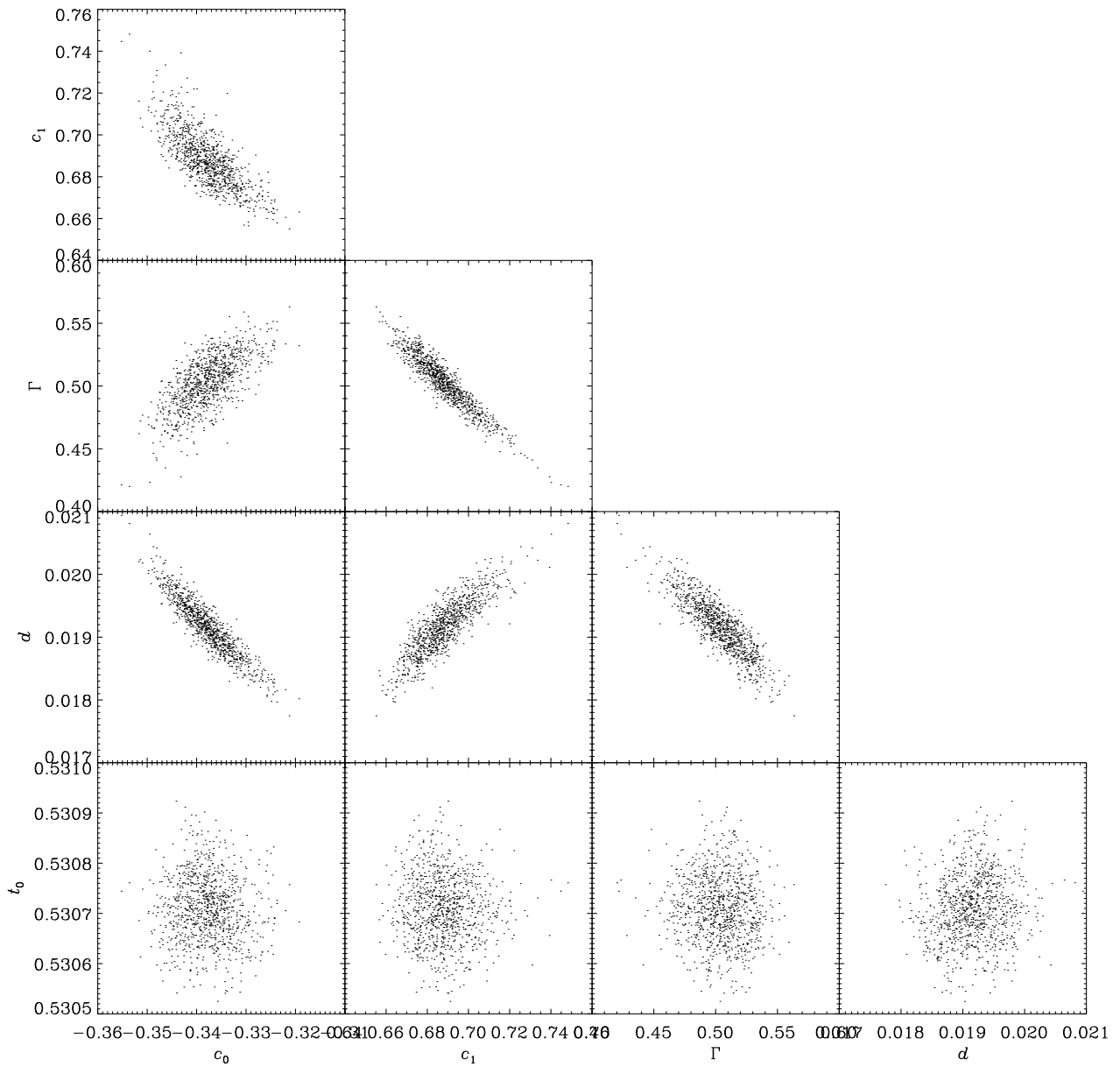


Figure 3: Correlations between individual parameters as determined by bootstrapping of data from Figure 1. The time of minimum  $t_0$  has little correlation with other parameters. This would not necessarily be true if we included also a linear in the form of  $c_2 t_i$  in Equation (2).